TOPICAL REVIEW — Magnetism, magnetic materials, and interdisciplinary research

Optimizing and fabricating magnetocaloric materials*

Liu Jian(刘 剑)†

Key Laboratory of Magnetic Materials and Devices, Ningbo Institute of Material Technology and Engineering, Chinese Academy of Sciences, Ningbo 315201, *China*

(Received 21 January 2014; published online 20 March 2014)

The microstructural modification of existing materials for magnetic cooling applications, and mass fabrication of the modified materials are reviewed, emphasizing the maximization of magnetic entropy change and minimization of hysteresis losses, as well as the engineering problems in the actual application of promising materials. In the first part, physical rules are put forward to explore high performance magnetic refrigerants, including the enhancement of adiabatic temperature change in finite field, multi-caloric effects, and multi-layered structure. Special attention is given to non-magnetic properties. Following this, an overview of mass fabrication of magnetic refrigerants having large entropy change, small hysteresis, good mechanical properties, and high thermal conductivity is presented.

Keywords: magnetocaloric effect, hysteresis, microstructure

PACS: 75.30.Sg **DOI:** 10.1088/1674-1056/23/4/047503

1. Introduction

Magnetic cooling is a novel, energy-efficient, and environmentally friendly technology that is targeted to replace conventional vapor-compression technology for air-conditioning, space heating, and the refrigeration of food (supermarket chillers, food processing plants, home refrigerator/freezers). It is based on the magnetocaloric effect (MCE), which occurs in magnetic materials, in particular those undergoing a magnetic or magneto-structural phase transition.[1–3] The field received a surge of interest in 1997 when Pecharsky and Gschneidner at Ames Lab, USA discovered a so-called giant magnetocaloric effect in $Gd_5Si_2Ge_2$ alloys around ambient temperature. The large MCE was due to coupled magnetic and structural transitions which are of first-order phase, and this could be induced by applying a magnetic field. Before this time gadolinium metal was the main candidate material, but it has a smaller MCE — a purely second-order magnetic transition without structural transition. Since that time, several intermetallic material systems with giant MCE have been discovered and developed, including $NaZn_{13}$-structured $La(Fe,Si)_{13}$-based alloys,[4,5] Fe_2P-structured MnFeP(As,Ge,Si) alloys,[6–8] and Ni–Mn-based Heusler alloys.[9] A comparison of magnetocaloric properties (here, adiabatic temperature change ΔT_{ad}) for near-room temperature magnetic refrigerants is shown in Fig. 1.[10] In general, the refrigerants transformed by magnetism-structure coupling (marked with solid fill-pattern) have a large MCE. Given this, we know that one way forward in the development of more efficient magnetic refrigerants is a focus on maximizing the structural (lattice) contribution to the total entropy change in moderate magnetic fields. This, however, has proven to be difficult engineer without introducing unwanted side-effects, such as hysteresis. Although early prototypes for demonstrating magnetic cooling incorporated gadolinium metal as the benchmark refrigerant, nowadays engineers have started to implement active magnetic regenerators (AMR) using $La(Fe,Co,Si)_{13}$ and MnAs alloys.[11–14] However, the remaining major challenges, especially for giant MCE materials, are the difficulties that arise in fast mass fabrication (due to multi-phase selective formation) and in shaping very thin refrigerant plates (due to the intrinsic brittleness of intermetallics). Several recent publications[3,15–17] and a viewpoint-set issue[18] review the selection of MCE materials and related physical properties. The present review paper will focus on the current approaches to explore the new magnetic materials with a large MCE, to maximize MCE and minimize hysteresis losses of existing materials by microstructural modification, and to solve the engineering problems of applications.

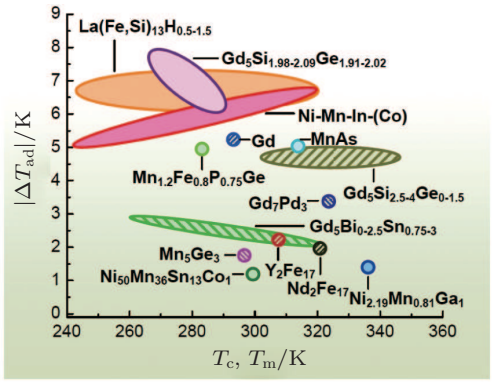


Fig. 1. Adiabatic temperature change ($\Delta H = 2$ T) for several of the most researched ambient magnetic refrigerants at either a purely magnetic transition temperature T_c (second-order transition, marked by hatched pattern) or magnetostructural coupling transition temperature T_m (first-order transition, solid fill-pattern).[10]

*Project supported by the Funds from the Thousand Young Talents Program of China, the Program of the Innovation Team of Ningbo City, and the National Natural Science Foundation of China (Grant No. 51371184).

†Corresponding author. E-mail: liujian@nimte.ac.cn

© 2014 Chinese Physical Society and IOP Publishing Ltd

2. Optimizing magnetocaloric alloys

2.1. Physical rule to explore high-performance magnetic refrigerants

2.1.1. Strategy to maximize adiabatic temperature change

The performance of a magnetocaloric materials depend mainly on two material parameters: the temperature change (ΔT_{ad}) when a magnetic field is applied to the material under adiabatic conditions and the entropy change (ΔS) under isothermal conditions. A good magnetic refrigerant should have large values for both parameters. Giant MCE materials have a strong coupling between their crystallographic structure and their magnetic behavior whereby a magnetic field can induce simultaneous changes of magnetic and lattice entropies. For example, in $Gd_5Si_2Ge_2$, a magnetic field-induced transformation from the paramagnetic monoclinic phase to the ferromagnetic orthorhombic phase brings about a giant MCE, wherein the lattice entropy change due to structural transition contributes more than half of the total entropy change ΔS.[19] Another example can be found in Ni–Mn-based Heusler alloys. These materials cool when magnetized and heat when demagnetized. This so-called "inverse MCE" originates from a dominant structural transition from the paramagnetic/antiferromagnetic martensite phase to the ferromagnetic austenite phase upon the application of a magnetic field.[9] As the absolute amount of heat absorption due to the structural transition exceeds that of heat release arising from the change of the magnetic subsystem, the net temperature decreases upon magnetization. Figure 2 schematically illustrates the different contributions to the total MCE in the case of inverse MCE.

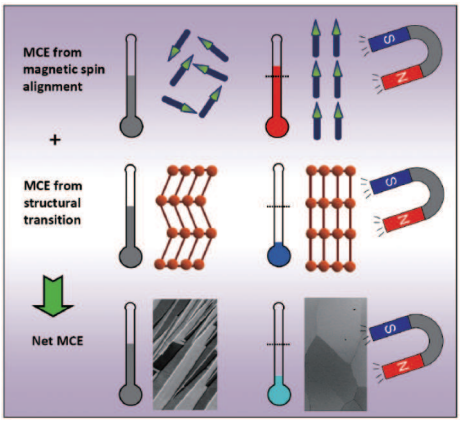


Fig. 2. Contributions from the magnetic and structural parts for a first-order magnetic transition to the MCE. The Ni–Mn-based martensitic transition alloy is used as an example.[10]

The most important parameter to directly assess a refrigerant's potential is the adiabatic temperature change. A roadmap for comparing normal and giant MCE materials with room-temperature operating ranges is shown in Fig. 3, taken from Sandeman.[20] A key physical parameter, field dependence of transition temperature (dT_c/dH), has been proposed to estimate the potential ΔT_{ad}. For instance, for the La–Fe–Si compounds, an optimum ΔT_{ad} is 13 K in 2 T when dT_c/dH is 6.5 K/T. In fact, such a giant value of ΔT_{ad} is hard to achieve, because real transition behavior differs from Sandeman's ideal model. For typical laboratory timescales, the transition occurs in some finite temperature range rather than at a well-defined specific temperature. In particular, the martensitic transition proceeds inhomogeneously owing to a local variation of composition, internal stresses, lattice defects, and atomic ordering. Also, the finite width of the transition might mean that applying a field cannot fully induce the transition and thus significantly reduces ΔT_{ad}. Therefore, the ΔT_{ad} is not manipulated solely by dT_c/dH. A phenomenological model that realistically describes the cooling effect in a finite change of magnetic field was established very recently for Ni–Mn–In–(Co).[10] For the development of novel magnetocaloric materials, to achieve a giant ΔT_{ad}, this general rule can be employed: a full phase conversion takes place when these three conditions are satisfied: (i) a narrow temperature range, (ii) high temperature, and (iii) a moderate field dependence of the transition temperature.

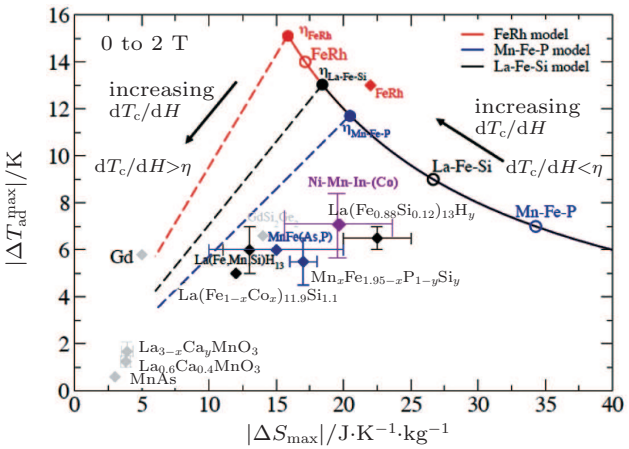


Fig. 3. Crucial variables for magnetocaloric performance ΔT_{ad}^{max} versus ΔS^{max} for materials exhibiting a large MCE at room temperature. Diamonds represent experimental values, potential ΔT_{ad}^{max} and ΔS^{max} are represented by hollow circles.[20] Copyright 2012, Elsevier.

2.1.2. Hysteresis issue and multi-caloric effect

Giant MCE materials usually display field hysteresis and thermal hysteresis, which are connected with losses that reduce the efficiency of the magnetic cooling cycle. The hysteresis also contributes ambiguity to the determination of the magnitudes of ΔT_{ad} and ΔS.[21] It is evident therefore that the information on hysteretic features and irreversibility of the magnetocaloric materials is extremely important for the construction of efficient prototype magnetic refrigerators. Marten-

sitic alloys are now typically taken as the subject for theoretical and experimental study of the hysteresis behavior, which can be manipulated by the lattice compatibilities of martensite and austenite phases, as well as by applying stimuli other than magnetic field. The geometric nonlinear theory of martensites suggests that their reversibility of structural transition critically depends on the crystalline symmetry and geometric compatibilities of the martensite and austenite phases. Therefore, the transition distortion matrix and its corresponding middle eigenvalue reflect hysteresis behavior. This principle has been adapted to search shape-memory alloys with zero hysteresis.[22–24] By this quantitative approach, a suitable composition has to be determined to satisfy the lattice conditions for eliminating the stressed transition layer during phase transformations. A further step to achieve even stronger compatibility conditions called the cofactor conditions has been proposed for achieving ultrahigh reversibility in Au–Cu–Zn alloys.[25]

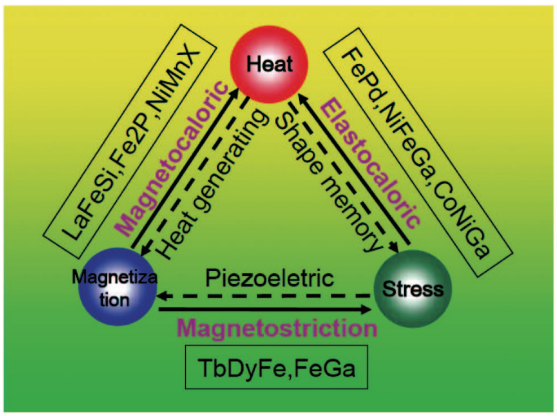


Fig. 4. A schematic plot to show energy conversions of multi-functional magnetic materials.

On the other hand, interest has been increasing in the multi-caloric effects in ferroic materials (the all-inclusive term for ferroelastic shape-memory alloys, ferromagnetic shape-memory alloys, and ferroelectric materials). By applying external magnetic, electric, elastic or hydrostatic fields, giant magneto-, electro-, elasto-, and baro-caloric effects have been obtained.[26] More broadly speaking, for ferroic materials, the energy conversion in various energy-driven sources — including magnetization, heat, and stress — is available, yielding multiple functionalities such as solid-state refrigeration, electricity generation, magnetostriction, and so on, as schematically shown in Fig. 4. It has been demonstrated that the utilization of different external stimuli is a feasible approach to manipulate structural transformation and associated hysteresis. As shown in Fig. 5, for $Ni_{50}Mn_{34}In_{16}$,[27] the application of pressure has a significant effect on the magnetic behavior in the temperature region where austenite and martensite coexist. The martensitic transformation temperatures shift to higher values with increasing pressure. The change in the magnetization between the martensite and austenite becomes larger with increasing pressure. Such an increase is consistent with the fact that the martensitic transition is shifted to higher temperatures, and along with this, the Curie temperature of martensite decreases. The pronounced increase of structural transformation temperature by applying relatively low hydrostatic pressures opens up a broad range of potential applications of magneto- and baro-caloric properties of the Ni–Mn-based Heusler alloys. Besides, when an $Ni_{45.2}Mn_{36.7}In_{13}Co_{5.1}$ sample is magnetized without bias stress but demagnetized under a moderate external hydrostatic pressure, the magnetic hysteresis is significantly reduced.[10]

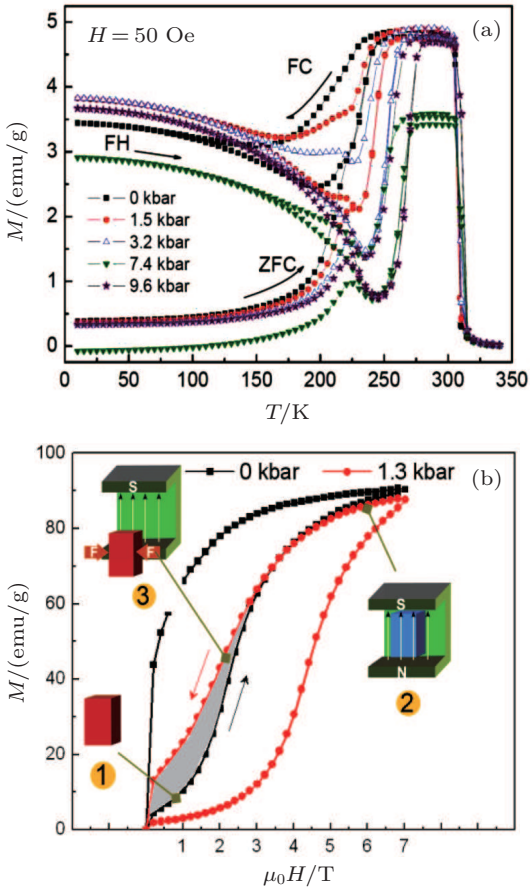


Fig. 5. (a) Low field M–T curves for selected applied pressures of $Ni_{50}Mn_{34}In_{16}$;[27] (b) M–T curves under 0 and 1.3 kbar hydrostatic pressure at 308 K for $Ni_{45.2}Mn_{36.7}In_{13}Co_{5.1}$. The forward and reverse transitions can be induced in a relatively low field (with little hysteresis: shaded region) when the sample is magnetized in zero pressure but demagnetized under an external pressure. This process is demonstrated schematically as well.[10] Copyright 2008, American Institute of Physics. The units 1 Oe = 79.5775 A·m^{-1} and 1 bar = 10^5 Pa.

2.2. Cascade magnetic refrigerants with tunable transitions

Sharp first-order magnetic transitions always imply a narrow refrigeration operating temperature range and therefore

limit the cooling span of a single magnetic refrigerant in AMR systems. This requires a stack of different materials but with an easily and finely tailored magnetic character, finally forming a cascade alloy system, which can be achieved either through varying the composition or by tuning the structural order.[10] If the fraction of each component is optimum, a 'table-like' curve of ΔS or ΔT_{ad} as a function of temperature can be observed. The composition of several kinds of alloy layers has been demonstrated to yield the most suitable characteristics for the ideal Ericsson cycle.[28] On the basis of such a consideration, the multi-layered structure has been used for the hydrogen liquefaction as well as room-temperature AMR.[29–31] Figure 6 collects the most promising magnetic refrigerants with a giant MCE (present here ΔT_{ad}) over a wide temperature range from 340 K to 10 K.[32–37] The materials shown here are all rare-earth-based alloys. Although Ni–Mn-based alloys also have a giant ΔT_{ad} about 7 K in 2 T,[10] their irreversible transition is still a bottleneck for practical applications. The giant MCE materials of MnFeP(Ge, Si) have large ΔS values, but their ΔT_{ad} measurements are rarely reported, so these materials are excluded from this figure. Note that in 100 K–150 K, no systems have been found to display superior MCE properties. Although the magneto-structural transition of $Ge_5Si_1Ge_3$ occurs in this range, it is accompanied by a large hysteresis. In the future, researchers need to focus on searching for a better materials to fill this gap. Generally, Gd-based binary alloys and La(Fe, Si)$_{13}$H-based alloys are highly likely to be applicable in a room-temperature cooling system, by virtue of their multiple Curie temperatures. To tune the Curie temperature of La–Fe–Si-based grade alloys, full hydrogenation followed by partial dehydrogenation has been adopted very often.[38] Partial dehydrogenation as a way to tune T_c is not very useful as it leads to instability and it is difficult to adjust precisely.[39] Instead, Mn-containing hydrogenated La(Fe, Mn, Si)$_{13}H_x$ is stable when working near to T_c and is a proven method to achieve a series of compositions to form a cascade of MCE materials with an extended operating temperature range.[37,40]

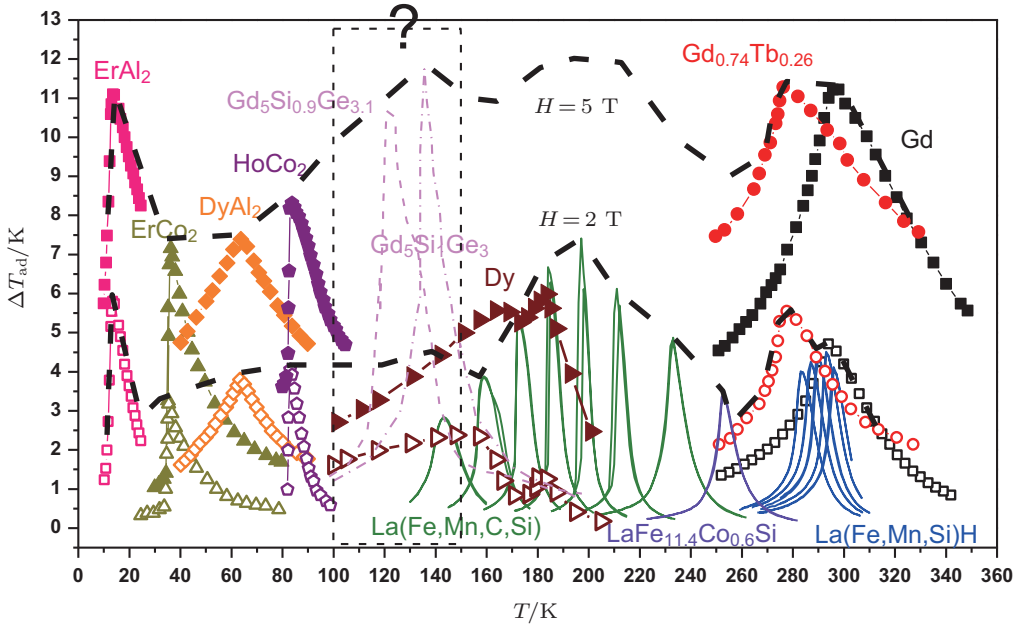


Fig. 6. Giant magnetocaloric materials with magnetic transitions over the entire temperature range. Herein the data of adiabatic temperature change are from the literature sources listed below: Gd, Dy, $HoCo_2$ — Tishin A M, *Handbook of Magnetic Materials*, North Holland, Amsterdam 1999;[32] $ErAl_2$, $DyAl_2$ — Ranke P J *et al.* 1998 *Phys. Rev. B* **58** 12110;[33] $ErCo_2$ — Wada H 1999 Cryogenics **39** 915;[34] $Gd_{0.74}Tb_{0.26}$ — Gschneidner K A 2000 *Mater. Sci. Eng. A* **287** 30;[35] $Gd_5Si_1Ge_3$, $Gd_5Si_{0.9}Ge_{3.1}$ (large hysteresis) — Pecharsky V K 1998 *Adv. Cryog. Eng.* **43** 1729;[36] LaFeSi-based — Liu J *et al.* 2012 *Scripta Mater.* **67** 584.[37]

2.3. Non-magnetic factors

Apart from magnetic phenomena, e.g., ΔS, ΔT_{ad}, and hysteresis, involved in the performance of AMR systems, a comprehensive assessment of magnetic refrigerants has to be taken in account, including the shape demagnetization factor, thermal conductivity, electrical resistivity, mechanical properties, life time (fatigue during cycling), and chemical stability when exposed to the corrosive conditions of working fluids.

(i) Demagnetization factor: A significant dependence of Gd MCE on the sample's orientation has been observed, which can be explained in terms of the demagnetization factor.[41]

(ii) Thermal conductivity: It is interesting to see that in case for a long flat refrigerant plate with isotropic thermal conductivity, high thermal conductivity is preferred when an AMR system is operated at a high frequency (> 2 Hz), but a

smaller conductivity favors the AMR when operating at low frequency (< 1 Hz), due to conduction losses along the long plate direction.[42] An ideal regenerator solid material should have anisotropic conductivity to enable transferring heat from the interior of the solid to the fluid while minimizing conduction losses inside the solid.

(iii) Electrical resistivity: When metallic magnetic refrigerants move into and out of a magnetic field, eddy currents are inevitably induced, which bring about unwanted heating of the magnetic refrigerant. Moreover, eddy currents can generate electromagnetic forces which form a strong braking effect. The higher is the electrical resistivity, the lower are the eddy currents. A little research has been done in terms of electrical resistivity for Gd (131 μΩ·cm) and La(Fe, Co, Si)$_{13}$ alloys (100 μΩ·cm–150 μΩ·cm) at room temperature.[43]

(iv) Mechanical properties: As most magnetic refrigerants are brittle intermetallic alloys — especially the hydrogenated La(Fe, Si)$_{13}$ alloys — the mechanical endurance against high forces (up to a hundred newtons) due to magnetization/demagnetization has become the central issue in applications of magnetic cooling materials. In particular, when the bulk sample is fabricated into refrigerant plates less than 1 millimeter thick, the excellent mechanical properties are of great importance for running AMR machines. Currently, more and more efforts are made to open up this bottleneck. More details about improved ductility will be presented in Section 3 of this paper.

(v) Life time: A common problem with first-order materials is that they undergo large volume changes and hence are prone to instability and fatigue problems. Fatigue is likely to occur when magnetic refrigerants are subjected to repeated magnetization and demagnetization. Microscopic cracks could lead to degrading MCE. Making porous/metal foam structures has been shown to greatly improve the resistance to cycling-fatigue, as the pores release internal strain.[44,45]

(vi) Corrosion: The chemical stability of rare-earth-based elements/compounds has been studied. NaOH solution was shown to be a good inhibitor to prevent Gd from being severely corroded.[46] The use of a mixture of Na_2MoO_4 and Na_2HPO_4 solution as a corrosion inhibitor was reported to decrease the corrosion rate of La(Fe, Si)$_{13}$.[47,48]

3. Fabricating and shaping magnetic refrigerants

3.1. Rapid solidification

Rapid solidification has been widely used for preparing La–Fe–Si-based alloys. The $NaZn_{13}$-type 1:13 phase does not develop readily in bulk material prepared by conventional melting methods (e.g. arc and induction melting). To obtain a single 1:13 phase, the ingot has to be subjected to a homogenization treatment at high temperatures (above 1100 K) for at least one week followed by quenching.[49] Alternatively, melt spinning and strip casting have been proposed to produce La(Fe, Si)$_{13}$ ribbon and flake materials, respectively.[50,51] It was found that only a quick (e.g. a few hours) heat treatment is required for melt-spun ribbons or strip-cast flakes, resulting in the formation of a more uniform microstructure and homogeneous element distribution during rapid solidification. Compared with the melt spinning technique, which normally has a mass limit, we recently pointed out that strip casting method has great potential for kilogram-scale production of high performance magnetocaloric materials.[52] In addition, to achieve a good heat transfer capability under a high operating frequency, micro-sized spherical particles and wires have also been prepared by rapid solidification.[53,54] Figure 7 presents the microstructural comparison for $LaFe_{11.6}Si_{1.4}$ in different forms. Cooling at a relatively slow rate (100 K/s), arc-melted bulk has coarse α-Fe dendrites about 40-μm long. The microstructure is gradually refined when the cooling rate increases; therefore the time required for homogenization is shortened.

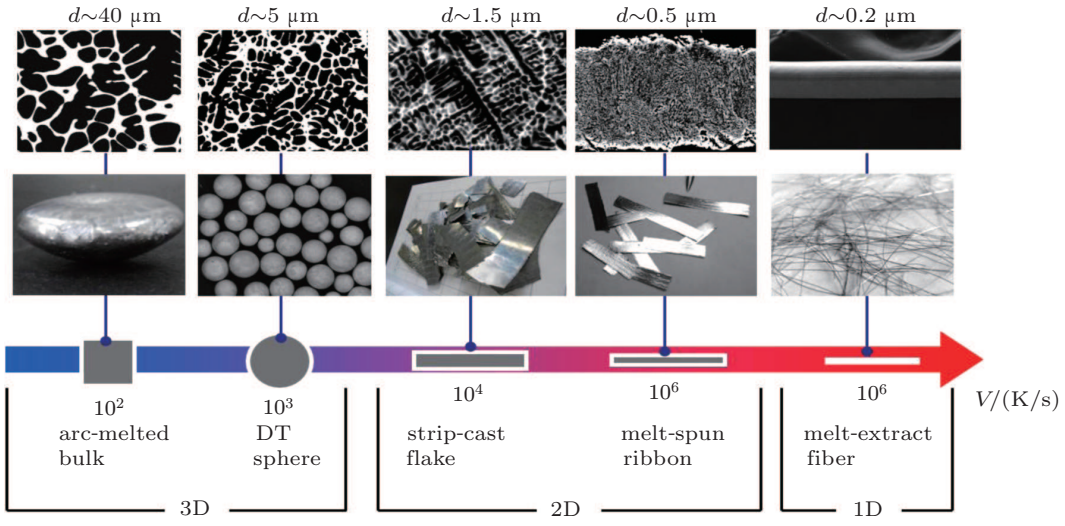


Fig. 7. Evolution of microstructure with various cooling rates for $LaFe_{11.6}Si_{1.4}$. DT represents drop tube method.

3.2. Powder metallurgical processing

Rapidly solidified ribbons and flakes cannot be directly used in AMR machines as they have to be consolidated into specific geometries, but they can be ground into fine powders as precursors for power metallurgy. Since Vacuumschmelze GmbH initially developed sintered La–Fe–Si-based blocks,[55] power metallurgy processing has been developed as an attractive technique in fabricating magnetic refrigerants. Besides, mechanical alloying followed by solid-state sintering is a conventional route for preparing Fe_2P-typed materials. We also note that the influence of powderization on the phase transition and magnetocaloric properties has been investigated for nanostructured Gd–Si–Ge and Co–Mn–Ge alloys.[56,57] As the MCE is rather sensitive to the particle size effect for the first order transition materials, the build-up of defects by severe plastic deformation would eliminate the metamagnetic transition and decrease related MCE.[37] In the following, the main route of power metallurgy will be introduced by taking La–Fe–Si and Mn–Fe–P–Ge alloys as examples.

3.2.1. Mechanical alloying

Mechanical alloying (MA) names synthesis of intermetallics from the elemental powders of their constituents. The main reason to employ mechanical alloying for MCE materials is the difficulties of melting methods for toxic or volatile elements, e.g. As and P. Most often, MA followed by solid-state sintering has been employed to prepare Mn–Fe–P–(Ge, Si) solid compounds.[58,59] This process normally takes about one week for homogenization. Alternatively, to shorten the consolidation time of Mn–Fe–P–Ge compounds, the spark plasma sintering (SPS) technique has been employed after MA.[60] Nevertheless, the time to form Fe_2P-type phase upon MA has not been effectively shortened, so the MnO impurity is likely to be present in the final alloys. Phejar *et al.* have started the investigation of preparation routes for La–Fe–Si compounds through MA, and gained $LaFe_{13-x}Si_x$ ($x = 1.4$, 1.6, 1.8, 2.0) ball-milled and 30-min annealed powders with MCE properties comparable to those in the bulk materials.[61] It is important to see that unlike milled compound powders having a heavily decreased MCE, $LaFe_{13-x}Si_x$ powders resulting from MA are still active. Probably, MA is the only suitable approach to synthesizing La–Fe–Si fine powders with a size lower than 10 μm and a high MCE.[37]

3.2.2. Liquid reactive sintering and TDR process

In the key sintering step of powder metallurgy for La–Fe–Si, the process has to be controlled above the melting temperature of excess La. This treatment is aimed to achieve full density of finished products. Figure 7(a) shows the scattered electron (BSE) SEM image of the microstructure of fully sintered $LaFe_{10.7}SiCo_{1.3}$.[62] Note that the La-rich phase segregates along the grain boundaries. As there is a giant thermal expansion for the $NaZn_{13}$-type phase when passing its Curie point, local temperature gradients around the cutting tool would lead to the formation of micro-cracks. A process named thermally induced decomposition and recombination (TDR) was proposed to overcome this problem for La–Fe–(Co)–Si.[63] In the course of the TDR process, the La(Fe, Co, $Si)_{13}$ phase decomposes to a lamellar structure consisting of α-Fe and 1:1:1 phases, as seen in Figs. 7(b) and 7(c), by a eutectoid-type phase transition at 873 K–1173 K.[62] The decomposed phases have highly enhanced mechanical properties and allow easier machining. Finally, the La(Fe, Co, $Si)_{13}$ phase can be fully recovered by annealing decomposed and well-machined thin plates around 1323 K.

3.3. Composites

In order to build an overall structure with good comprehensive characteristics, high conductivity metal (copper or silver) or polymer resin is combined with MCE particles. An innovation has been developed to form La(Fe, $Si)_{13}$/Cu composites using electroless deposition from aqueous solutions, in which the Cu coating thickness is controllable and better thermal conductivity is obtained for the composites.[64] Though the mechanical properties were not reported, the crack formation may likely occur due to the relatively higher percentage of pores (about 25 vol.%). The corrosion resistance was improved by coating Cu for $LaFe_{11.5}Si_{1.5}$.[65] Using Ag impregnation, the thermal conductivity of manganites was increased 3 fold, up to 2.5 W/mK.[66] To overcome the inherent brittleness of intermetallic alloys, one solution is the use of metal particles suspended in a stiffness-matched polymer matrix. The polymer-bonded functional magnetic materials have been studied in Ni–Mn-based magnetic shape memory (MSM) composites.[67,68] The criteria for polymer selection and the interface of MSM particles and polymer are of importance to preserve the field-driven actuation behavior of Ni–Mn–Ga. As for the polymer-bonded MCE composites, other essential issues, e.g. thermal conductivity and constraint effect of polymer, have to be taken into consideration. Compacting $LaFe_{11.6}Si_{1.4}$ particles with 5 wt% silver epoxy under a pressure of 0.1 GPa leads the production of 0.6-mm thick plates, which can be stacked and glued into a porous heat exchanger.[69] Higher pressure however resulted in a dramatic reduction of MCE as initial grains cracked into fragments with the size less than 10 μm. To the best of my knowledge, the hot pressing technique has not been adapted in fabrication of metal reinforced magnetic refrigerants. The present author's group is currently aiming to explore novel La–Fe–Si-based composites by structuring the MCE matrix wrapped with ductile and high-conductive metals. The high thermal conductivity can be realized by building continuous connection of introduced metals, while the pores release internal strain, thus greatly improving the resistance to cycling-fatigue. In addition, the corrosion problem can be simultaneously solved by corrosion resistant metals that isolate the matrix from the heat exchange liquid. Figure 8 shows the microstructure of La–Fe–Si/Al composites obtained by hot pressing.

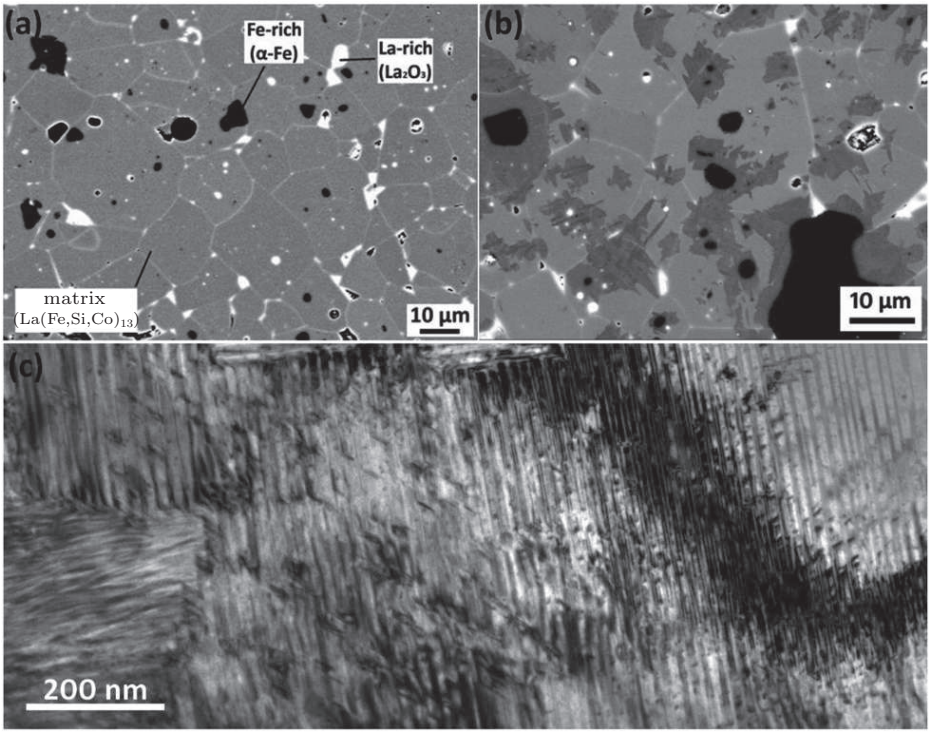


Fig. 8. Back scattered electron (BSE) images of the microstructure of fully sintered $LaFe_{10.7}SiCo_{1.3}$ before (left) and after (right) ageing at 973 K for 4 h. Panel (c) shows a TEM image for lamellas.[62]

3.4. Shaping challenges

A typical AMR machine requires thin plates of refrigerants with thicknesses well below 0.5 mm, which makes the machining of intermetallic alloys a significant challenge. The above mentioned TDR process allows cutting La–Fe–Co–Si into plates in this thin range. However, precise cutting is still costly and time consuming. A regenerator structure for AMR can be designed by aligning MCE material plates parallel to each other, or by manufacturing micro-channels in a block.[70] For the latter, it is necessary to tailor the optimum number, shape, and size of channels spread uniformly over a given volume of the refrigerant matrix. These parameters are vital to maximum the cooling powder and avoid large pressure drops. The sophisticated geometries have been made by selective laser melting (SML) technique. Figure 9 shows two demonstrations of SML created $LaFe_{11.7}Co_{1.3}Si$ blocks with wavy-channel geometry and fin-shaped rods.[71] Other ways to produce thin plates, such as extrusion, rolling, and forging have been reviewed previously.[37]

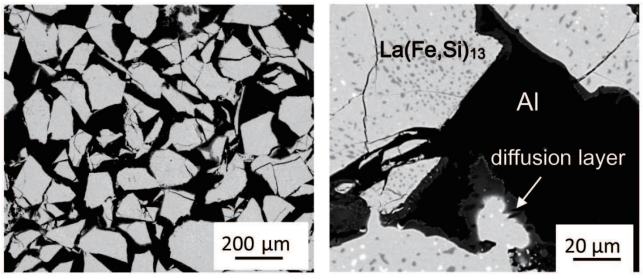


Fig. 9. Back scattered electron (BSE) images of the microstructure of hot-pressed $LaFe_{11.6}Si_{1.4}$/Al composites.

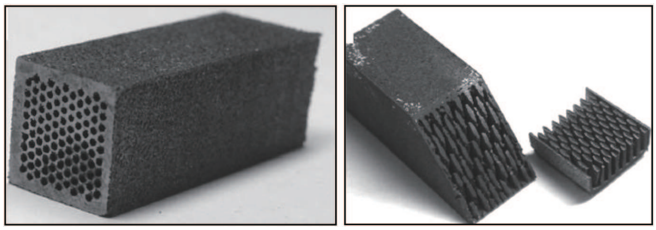


Fig. 10. $LaFe_{11.7}Co_{1.3}Si$ blocks with wavy-channel geometry (left) and with fin-shaped rods (right).[71] Copyright 2013, American Institute of Physics.

4. Extension remarks

This review paper has purely highlighted the recent developments, the current trends, and the new strategies for magnetocaloric materials. With the acceptance of the new alternative cooling method by the refrigeration community, the commercialization of magnetic cooling technique has to be pushed harder. This definitely does not depend only on the contribution of magnetocaloric material development and research. Future perspectives of the modeling simulation on thermal characterization and magnetic circle design, and the promotion of smarter and more efficient AMR machines are of the same importance. The International Conference on Magnetic Refrigeration at Room Temperature (THERMAG) has been held five times. In previous years the scope covered room-temperature magnetocaloric materials, modeling, and systems. THERMAG VI will be open in 2014 at the Victoria Conference Centre, Canada, and has announced an enhanced scope

that includes all magnetocaloric materials and applications, regardless of temperature range. This allows for coverage of new applications such as gas liquefaction systems as well as thermally driven magnetic heat engines. From this point of view, magnetic cooling techniques will be advanced in much wider application fields. Whether they work at ambient temperature or in cryogenic conditions, optimizing and fabricating magnetocaloric materials are invariable concepts. Therefore, we believe that the presently mentioned approaches to enhance the physical, chemical, mechanical, and thermal properties of MCE alloys provides a worthwhile reference to the magnetic cooling community.

Acknowledgments

The author is grateful to M. X. Zhang, J. D. Dong and A. R. Yan for experimental assistance. O. Gutfleisch, K. Skokov, J. Moore and M. Krautz are acknowledged for scientific support and fruitful discussion during the author's work at the IFW Dresden.

References

[1] Gschneidner K A Jr, Pecharsky V K and Tsokol A O 2005 *Rep. Prog. Phys.* **68** 1479
[2] Gutfleisch O, Willard M A, Bruck E, Chen C H, Sankar S G and Liu J P 2011 *Adv. Mater.* **23** 821
[3] Shen B G, Sun J R, Hu F X, Zhang H W and Cheng Z H 2009 *Adv. Mater.* **21** 4545
[4] Hu F X, Shen B G, Sun J R, Cheng Z H, Rao G H and Zhang X X 2001 *Appl. Phys. Lett.* **78** 3675
[5] Fujieda S, Fujita A and Fukamichi K 2002 *Appl. Phys. Lett.* **81** 1276
[6] Tegus O, Bruck E, Buschow K H J and de Boer F R 2004 *Nature* **415** 250
[7] Trung N T, Ou Z Q, Gortenmulder T J, *et al*. 2009 *Appl. Phys. Lett.* **94** 102513
[8] Dung N H, Ou Z Q, Caron L, *et al*. 2011 *Adv. Energy Mater.* **1** 1215
[9] Krenke T, Duman E, Acet M, Wassermann E F, Moya X, Manosa L and Planes A 2005 *Nat. Mater.* **4** 450
[10] Liu J, Gottschall T, Skokov K, Moore J and Gutfleisch O 2012 *Nat. Mater.* **11** 620
[11] Zimm C, Boeder A, Chell J, Sternberg A, Fujita A, Fujieda S and Fukamichi K 2006 *Int. J. Refrig.* **29** 1302
[12] Sari O and Balli M 2014 *Int. J. Refrig.* **37** 8
[13] Tusek J, Kitanovski A, Tomc U, Favero C and Poredos A 2013 *Int. J. Refrig.* **37** 117
[14] Moos L, Nielsen K K, Engelbrecht K and Bahl C R H 2014 *Int. J. Refrig.* **37** 303
[15] Roy S B 2013 *J. Phys.: Condens. Matter* **25** 183201
[16] Smith A, Bahl C R H, Bjok R, Engelbrecht K, Nielsen K K and Pryds N 2012 *Adv. Energy Mater.* **2** 1288
[17] Franco V, Blazquez J S, Ingale B and Conde A 2012 *Ann. Rev. Mater. Res.* **42** 305
[18] Gutfleisch O and Franco V 2012 *Scripta Mater.* **67** 521
[19] Pecharsky V K and Gschneidner Jr K A 2001 *Adv. Mater.* **13** 683
[20] Sandeman K G 2012 *Scripta Mater.* **67** 566
[21] Liu J, Scheerbaum N, Lyubina J and Gutfleisch O 2008 *Appl. Phys. Lett.* **93** 102512
[22] Cui J, Chu Y S, Famodu O O, *et al*. 2006 *Nat. Mater.* **5** 286
[23] Zarnetta R, Takahashi R and Young M L, *et al*. 2010 *Adv. Funct. Mater.* **20** 1917
[24] Srivastava V, Song Y T, Bhatti K and James R D 2011 *Adv. Energy Mater.* **1** 97
[25] Song Y T, Chen X, Dabade V, Shield T W and James R D 2013 *Nature* **502** 85
[26] Fähler S, Röbler U K, Kastner O, Eckert J, Eggeler G, Emmerich H, Entel P, Müller S, Quandt E and Albe K 2012 *Adv. Eng. Mater.* **14** 10
[27] Manosa L, Moya X, Planes A, Gutfleisch O, Lyubina J, Barrio M, Tamarit J L, Aksoy S, Krenke T and Acet M 2008 *Appl. Phys. Lett.* **92** 12515
[28] Smaili A and Chahine R 1997 *J. Appl. Phys.* **81** 824
[29] Hashimoto T, Kuzuhara T, Sahashi M, Inomata K, Tomokiyo A and Yayama H 1987 *J. Appl. Phys.* **62** 3873
[30] Paticopoulos S C, Caballero-Flores R, Franco V, Blazquez J S, Conde A, Knipling K E and Willard M A 2012 *Solid State Comm.* **152** 1590
[31] Engelbrecht K, Nielsen K K and Bahl C R H 2011 *Int. J. Refrig.* **34** 1132
[32] Tishin A M 1999 *Handbook of Magnetic Materials* (Amsterdam: North Holland)
[33] Ranke P J, Pecharsky V K and Gschneidner Jr K A 1998 *Phys. Rev. B* **58** 12110
[34] Wada H 1999 *Cryogenics* **39** 915
[35] Gschneidner K A Jr 2000 *Mater. Sci. Eng. A* **287** 30
[36] Pecharsky V K 1998 *Adv. Cryog. Eng.* **43** 1729
[37] Liu J, Moore J D, Skokov K P, Krautz M, Löwe K, Barcza A, Katter M and Gutfleisch O 2012 *Scripta Mater.* **67** 584
[38] Lyubina J, Gutfleisch O, Kuz'min M D and Richter M 2008 *J. Magn. Magn. Mater.* **320** 2252
[39] Krautz M, Moore J D, Skokov K, Liu J, Teixeira C S, Schafer R, Schultz L and Gutfleisch O 2012 *J. Appl. Phys.* **112** 083918
[40] Barcza A, Katter M, Zellmann M, Russek V, Jacobs S and Zimm C 2011 *IEEE Trans. Mag.* **47** 3391
[41] Nielsen K K and Bahl C R H 2009 *J. Appl. Phys.* **105** 013916
[42] Nielsen K K and Engelbrecht K 2012 *J. Phys. D: Appl. Phys.* **45** 145001
[43] Hu F X, Qian X L, Wang G J, Sun J R, Shen B G, Cheng Z H and Gao J 2005 *Chin. Phys.* **14** 2329
[44] Lyubina J, Schaefer R, Martin N, Schultz L and Gutfleisch O 2010 *Adv. Mater.* **22** 3735
[45] Chmielus M, Zhang X X, Witherspoon C, Dunand D C and Müllner P 2009 *Nat. Mater.* **8** 863
[46] Zhang Z Y, Long Y, Wen D, Ye R C and Wan F R 2004 *J. Rare Earths* **22** 99
[47] Balli M, Sari O, Zamni L, Robert A, Forchelet J and Fruchart D 2011 *Solid State Phenom.* **170** 248
[48] Zhang M, Ye R C, Long Y and Chang Y Q 2011 *J. Rare Earths* **29** 138
[49] Liu J, Krautz M, Skokov K, Woodcock T G and Gutfleisch O 2011 *Acta Mater.* **59** 3602
[50] Yan A, Muller K H and Gutfleisch O 2005 *J. Appl. Phys.* **97** 036102
[51] Hirosawa S, Tomizawa H and Bekki K 2006 *IEEE Trans. Magn.* **42** 3608
[52] Zhang M X, Zhang Y, Hu K, Yan A and Liu J (unpublished)
[53] Liu J, Zhang P N, Dai F P and Yan A 2013 *Scripta Mater.* **69** 485
[54] Dong J D, Yan A and Liu 2014 *J. Magn. Magn. Mater.* **357** 73
[55] Katter M, Zellmann V, Reppel G W and Uesuener K 2008 *IEEE Trans. Mag.* **44** 3044
[56] Trevizoli P V, Alves C S, Mendes M A B, Magnus A and Gama S 2008 *J. Magn. Magn. Mater.* **320** 1582
[57] Yuzuak E, Durak G, Dincer I and Elerman Y 2012 *J. Alloys Compd.* **541** 256
[58] Dagula W, Tegus O, Fuquan B and Zhang L 2005 *IEEE Trans. Mag.* **41** 2778
[59] Dung N H, Zhang L, Ou Z Q and Brück E 2012 *Scripta Mater.* **67** 975
[60] Yue M, Li Z Q, Wang X L, Liu D M, Zhang J X and Liu X B 2009 *J. Appl. Phys.* **105** 07A915
[61] Phejar M, Paul-Boncour V and Bessais L 2010 *Intermetallics* **18** 2301
[62] Löwe L, Liu J, Skokov K, Moore J, Sepehri-Amin H, Hono K, Katter M and Gutfleisch O 2012 *Acta Mater.* **60** 4268
[63] Katter M, Zellmann V, Reppel G W and Uestuener K 2009 in: Egolf P W, Brück E, Sandenman K G (ed.), *Proceedings of the Third International Conference on Magnetic Refrigeration at Room Temperature*, IIR, Des Moines, Iowa, 2009, p. 83
[64] Lyubina J, Hannemann U, Cohen L F and Ryan M P 2012 *Adv. Energy Mater.* **2** 1323
[65] Tian N, Zhang N N, You C Y, Gao B and He J 2013 *J. Appl. Phys.* **113** 103909
[66] Turcaud J A, Morrison K, Berenov A, Alford N, Sandeman K and Cohen L F 2013 *Scripta Mater.* **68** 510
[67] Liu J, Scheerbaum N, Kauffmann-Weiss S and Gutfleisch 2012 *Adv. Eng. Mater.* **14** 653
[68] Liu J, Scheerbaum N, Weiss S and Gutfleisch 2009 *Appl. Phys. Lett.* **95** 152503
[69] Skokov K P, Karpenkov D Y, Kuzmin, Radulov I A, Gottschall T, Kaesewurm B, Fries M and Gutfleisch O 2014 *J. Appl. Phys.* (in press)
[70] Vasile C and Muller C 2006 *Int. J. Refrig.* **29** 1318
[71] Moore J, Klemm D, Lindackers D, Grasemann S, Träger R, Eckert J, Löber L, Scudino S, Katter M, Barcza A, Skokov K and Grufleisch 2013 *J. Appl. Phys.* **114** 043907